minerals

MDPI

Article

Chronic Lead Exposure Alters Mineral Properties in Alveolar Bone

Pedro Álvarez-Lloret [1,*], Cristina Benavides-Reyes [2], Ching-Ming Lee [3], María Pilar Martínez [3], María Inés Conti [3], Alejandro B. Rodríguez-Navarro [4], Santiago González-López [2], Alberto Perez-Huerta [5] and Antonela Romina Terrizzi [3]

[1] Department of Geology, Faculty of Geology, University of Oviedo, 33005 Oviedo, Spain
[2] Department of Operative Dentistry, School of Dentistry, University of Granada, 18071 Granada, Spain; crisbr@ugr.es (C.B.-R.); sglopez@ugr.es (S.G.-L.)
[3] Department of Physiology, School of Dentistry, University of Buenos Aires, Buenos Aires C1122, Argentina; chingminglee@hotmail.com (C.-M.L.); pilar.martinez@odontologia.uba.ar (M.P.M.); maria.conti@odontologia.uba.ar (M.I.C.); anto_terri@hotmail.com (A.R.T.)
[4] Department of Mineralogy and Petrology, Faculty of Sciences, University of Granada, 18002 Granada, Spain; anava@ugr.es
[5] Department of Geological Sciences, University of Alabama, Box 870338, Tuscaloosa, AL 35487, USA; aphuerta@ua.edu
* Correspondence: pedroalvarez@uniovi.es

Abstract: The objective of the present study was to investigate the effects of chronic lead exposure on the mineral properties of alveolar bone. For this purpose, female Wistar rats ($n = 8$) were exposed to 1000 ppm lead acetate in drinking water for 90 days, while the control group ($n = 5$) was treated with sodium acetate. The alveolar bone structure and chemical composition of the dissected mandibles were examined using micro-computed tomography (micro-CT), scanning electron microscopy (SEM), inductively coupled plasma optical emission spectrometry (ICP-OES), attenuated total reflection Fourier transform infrared spectroscopy (ATR-FTIR), and X-ray diffraction (XRD) techniques to determine possible alterations in alveolar bone due to lead exposure. In addition, changes in bone mechanical properties were analysed using a three-point bending test. Exposure to lead induced notable changes in bone mineralization and properties, specifically a reduction of the trabecular thickness and bone mineral density. Furthermore, there was a reduction in carbonate content and an increase in bone mineral crystallinity. These changes in bone mineralization could be explained by an alteration in bone turnover due to lead exposure. Three-point bending showed a trend of decreased displacement at failure in the mandibles of lead-exposed rats, which could compromise the mechanical stability and normal development of the dentition.

Keywords: lead intoxication; alveolar process; bone mineralization; trabecular morphology; apatite crystallinity; mechanical properties

Citation: Álvarez-Lloret, P.; Benavides-Reyes, C.; Lee, C.-M.; Martínez, M.P.; Conti, M.I.; Rodríguez-Navarro, A.B.; González-López, S.; Perez-Huerta, A.; Terrizzi, A.R. Chronic Lead Exposure Alters Mineral Properties in Alveolar Bone. *Minerals* **2021**, *11*, 642. https://doi.org/10.3390/min11060642

Academic Editor: Jean-Pierre Cuif

Received: 14 March 2021
Accepted: 11 June 2021
Published: 16 June 2021

Publisher's Note: MDPI stays neutral with regard to jurisdictional claims in published maps and institutional affiliations.

Copyright: © 2021 by the authors. Licensee MDPI, Basel, Switzerland. This article is an open access article distributed under the terms and conditions of the Creative Commons Attribution (CC BY) license (http://creativecommons.org/licenses/by/4.0/).

1. Introduction

Alveolar bone is the part of the mandible that anchors and supports the teeth to the cementum via the periodontal ligament. This bone is a vascularized tissue formed by predominantly cancellous bone in the inner region surrounded by cortical bone in the outer layer [1]. Similar to other bones in the skeleton, alveolar bone is a highly mineralized tissue that consists of 60% inorganic phase in the form of hydroxyapatite crystals, 25% organic matrix (predominantly collagen type I), and 15% water [2]. Bone is a living tissue that plays an essential role in many metabolic processes, such as serving as an ion reservoir and absorbing and releasing elements needed for several cell functions [3]. Moreover, bone is a highly dynamic structure, continually forming and resorbing (i.e., bone turnover) in response to changing functional requirements and physiological conditions. The

mineral composition of bone is close to hydroxyapatite, $Ca_{10}(PO_4)_6(OH)_2$, but bone also incorporates many impurities, such as carbonate, sodium, zinc, and magnesium ions [4]. This lack of stoichiometry in biologically controlled precipitation causes bone apatite to have a high resorption rate, enabling bone remodelling processes. Bone metabolism is highly regulated by the organism, though it can be altered by several genetic factors, disease, nutrition, and environmental conditions such as exposure to pollutants.

Lead exposure has been associated with several bone mineral alteration

s and defective skeletal growth processes [5,6]. Due to its accumulative effect, 90%–95% of the total lead in the body is stored in the mineralized tissues (teeth and bones) because of its ability to substitute other divalent cations in the hydroxyapatite lattice, such as calcium, magnesium, and iron. Lead can directly affect the mechanisms of bone mineralization by interfering with the activity of osteoclasts and osteoblasts, but it can also indirectly affect these mechanisms by damaging organs (e.g., the kidneys) involved in calcium homeostasis [6]. The severe inhibition of calcium assimilation elicited by lead poisoning, together with the metabolic imbalances it causes, may lead to the development of different bone pathologies, such as osteoporosis [7,8]. These compositional and structural alterations have a direct influence on the bone mechanical properties, reducing their hardness and resistance to external stress and compromising their physiological function. Several studies have shown the toxic effects of lead exposure in bone mineralization by analysing its properties at different scales [5,9–11]. Many analytical techniques are available to assess mineral properties related to chemical composition (e.g., Fourier transform infrared and Raman spectroscopies) and microstructural characteristics (e.g., X-ray diffraction and electron microscopies) in bone health and disease [12–15]. Likewise, other techniques based on computerized tomography enable the study of the morphological properties of bone tissue (trabecular/cortical area and density) [16]. These techniques provide detailed information about bone structural organization, chemical composition, and mineral crystallinity, which provide critical contributions to bone properties (e.g., mechanical characteristics). To date, few studies have attempted to study the toxic effects of lead exposure on the alveolar bone, particularly the effects on bone properties at different scales.

The objective of the current research was to investigate the effects of chronic lead exposure on alveolar mineralization properties in the mandibles of rats. For this purpose, we employed the complementary analytical techniques of micro-tomography (micro-CT), scanning electron microscopy (SEM), optical emission spectroscopy (ICP-OES), attenuated total reflection infrared spectroscopy (Fourier transform infrared spectroscopy, ATR-FTIR), and X-ray diffraction (XRD) to carry out a comprehensive analysis of the alveolar bone structure and chemical properties. The study of the alterations due to lead exposure in the alveolar bone is important to evaluate the impact it may have on the development of the dentition and the mechanical response of the mandible. Furthermore, knowledge about the toxic effects of lead on different types of bones can improve the understanding of the development of bone diseases and dysfunctions.

2. Materials and Methods

2.1. Animals and Experimental Design

Protocols were approved by the Institutional Animal Care and Use Committee (no. 11/06/2012–23) of the Faculty of Dentistry, University of Buenos Aires (Argentina). Thirteen female Wistar rats (21 days old) from the animal facility of the Faculty of Pharmacy and Biochemistry (UBA, Argentina) were kept individually in stainless-steel cages and maintained under local vivarium conditions (22–23 °C, 12/12 h light/dark cycles). All animals were allowed free access to tap water (Pb < 0.005 ppm) and a standard pelleted chow diet (Pb-free) in accordance with international guidelines and standard ISO and WHO references. Rats were randomly divided into an exposure group (Pb) of 8 animals and a control group (C) of 5 animals. Pb intoxication was induced through the administration of 1000 ppm of lead acetate in tap water for 90 days [17]. This level of intoxication was

intentionally used to enable the creation of a model to evaluate Pb exchange between body compartments, particularly in bone tissue. The rate of lead exposure was approximately 21 mg Pb/day per animal, considering the average daily water intake of rats. To estimate how much lead was absorbed, lead content in the blood was analysed using an atomic absorption spectrophotometer. The animals of the control group received sodium acetate added to tap water during the same period. Rats were euthanized by unconscious decapitation and mandibles were properly dissected, cleaned from soft tissue, and stored at −20 °C until analyses. All animals were treated in accordance with the National Institutes of Health guidelines for the care and use of laboratory animals.

In order to identify the suitability of samples for further analysis, mandibles were inspected under an optical microscope to confirm the absence of microcracks or fractures before micro-CT, SEM, and mechanical testing. Subsequently, mandibles were sectioned and the alveolar bone was removed using an osteotome. Figure 1 shows a Wistar rat mandible with the reference directions highlighted. The methodology is described below according to the order of the techniques employed.

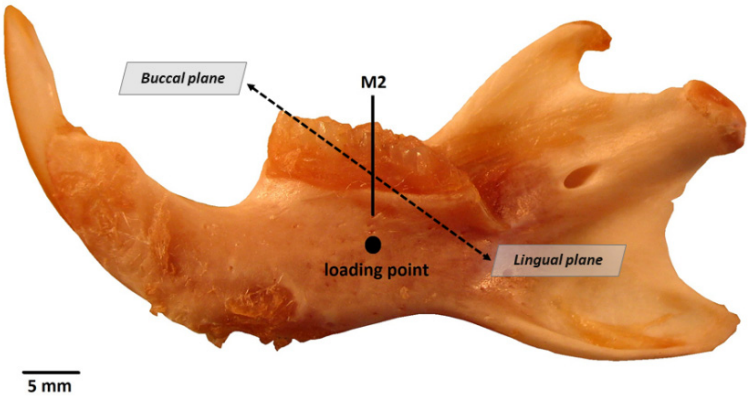

Figure 1. Mandible from a Wistar rat, control group specimen. M2, 2nd molar; loading point for the three-point bending test. Buccal and lingual planes are shown for reference.

2.2. Micro-CT Analyses

Micro-CT analyses of the right mandible were performed using a high-resolution microcomputed tomograph Skyscan CT-1174 (Skyscan, Bruker, Kontich, Belgium). The X-ray source was set at 50 kV and 800 mA, with a pixel size of 17 μm. For each specimen, 465 projection images were acquired over an angular range of 180° (angular step of 0.40°). Flat field correction was performed at the beginning of each scan. Due to the irregular alveolar bone morphology, the region of interest (ROI) was interactively delimited in each of the images for microarchitectural measurements. For the trabecular region, a total of 150 consecutive slices were selected, and adaptive grayscale threshold levels ranging from 78 to 250 were used. The image slices were reconstructed using the reconstruction software NRecon (Skyscan, Bruker, Kontich, Belgium). Morphometric analysis was based on the 2D and 3D internal CTAn plug-ins. After ROI determination, the images were converted for three-dimensional calculation. The following microarchitectural parameters were assessed: total volume (TV, mm^3), bone volume (BV, mm^3), bone volume/total tissue volume (BV/TV, %), apparent bone mineral density (BMD, mg/cm^3), trabecular thickness (Tb.Th, mm), trabecular separation (Tb.Sp, mm), trabecular number (Tb.N, mm^{-1}), and connectivity density (Conn.Dn, $1/mm^3$). A detailed description of the parameters employed here is described elsewhere [16,18].

2.3. Scanning Electron Microscopy (SEM)

The buccal axial planes of the mandibles were sequentially flattened with SiC papers (180-, 320-, 600-, 800-, and 1000-grit) and then polished with 1- and 0.3-μm aluminium

oxide pastes. After polishing, the specimens were cleaned by ultrasonication with deionized water, air dried, and coated with Au (10-nm thick coating) using ion sputtering equipment. Electron microscope imaging was carried out using a field emission scanning electron microscope (JEOL JSM-7000F, Peabody, MA, USA) housed at the Alabama Analytical Research Center (AARC) of the University of Alabama, operated under a 2.0×10^4 Pa vacuum at 20 kV voltage and a 10 mA current.

2.4. Three-Point Bending Test

The flexural strength was determined by a mechanical test machine (model 3345, Instron Co., Canton, MA, USA) using a 500 N load cell with a span length of 4.0 mm between points and a loading speed of 1 mm/min until sample fracture. The mandible was placed lingual side up, and the central loading point was aligned at the second molar midpoint (see reference loading point in Figure 1). To characterize the mechanical properties of the samples, the flexural strength (MPa, load applied) and extension by compression (mm, total movement of the load from the moment of contact with the surface until bone fracture) were determined at the moment of fracture.

2.5. Elemental Analyses

After the previously mentioned analyses, alveolar bone was removed using an osteotome and pulverized using a ball mill (Pulverisette 23, Fritsch, Idar-Oberstein, Germany). An aliquot of 30 mg powdered bone sample was dissolved in 1 mL of a solution of 70% HNO_3 for 24 h, followed by 1 mL of a solution of 30% H_2O_2 for 24 h, at room temperature. After digestion, 8 mL of Milli-Q water was added, and the solution was filtered. Calcium, phosphorus, and lead concentrations (in dry weight) were measured by an ICP-OES spectrometer (Optima 8300 Perkin Elmer, Waltham, MA, USA). The precision was higher than 1 ppm.

2.6. Attenuated Total Reflectance Infrared Spectrometry Analyses

Bone powdered samples were analysed by ATR-FTIR with a JASCO 6200 spectrometer equipped with a diamond crystal window (Pro ONE, JASCO, Japan). The ATR-FTIR spectra of powdered bone samples were recorded from 600 to 4000 cm^{-1} in absorbance mode at a 1 cm^{-1} resolution over 124 scans. The relative amounts of water, protein (mainly collagen), and phosphate and carbonate groups (i.e., mineral components) were determined from the corresponding peak areas of the absorption bands related to the characteristic molecular groups [12]. Overlapping peaks were resolved using the second derivative method, and the integrated areas were measured using curve fitting software (JASCO Spectra Manager, PeakFit v4.11). From the peak area measurements, the following compositional parameters were determined to quantitatively assess the bone mineral composition and crystallinity index parameters: (1) degree of mineralization, corresponding to the relative amount of mineral to organic matrix (PO4/Amide I), determined as the ratio of the main phosphate (υ_1, υ_3 PO_4; 900–1200 cm^{-1}) to Amide I band area (1590–1710 cm^{-1}) [12]; (2) carbonate to phosphate in the mineral, determined as the ratio between the main carbonate band (υ_3 CO_3; 1405 cm^{-1}) to the main phosphate band area (900–1200 cm^{-1}) [19,20]; and (3) crystallinity Index (CI), calculated from the υ_1, υ_3 PO_4 phosphate sub-band areas, determined as the ratio between 1030 cm^{-1} (high crystalline apatite phosphates) and 1020 cm^{-1} (poorly crystalline apatite phosphates) [21].

2.7. X-ray Diffraction Analyses

The X-ray diffraction pattern was obtained by using a powder diffractometer (X'Pert Pro, PANalytical, Almelo, The Netherlands) with Cu$K\alpha$ radiation produced at 40 mA and 45 kV. The scans were acquired between 20° and 75° (2θ values) with a step of 0.0042° and a counting time of 5.08 s per step. The average crystallite size (d) of the apatite-bone crystals was calculated from the (002) diffraction peak (apatite c-axis direction) by the Scherrer

equation [22]: $d_{(002)} = K \lambda / B \cos \theta$; where K is the broadening constant varying with crystal habit (chosen K = 0.9) [23], λ is the wavelength of CuKα radiation (λ = 1.5406 Å), B is the full width at half maximum (FWHM) for the (002) diffraction peak in radians, and θ is the corresponding diffraction angle. The width of a specific diffraction line represents a measure of the average coherent crystal size domains, employed as a crystallinity index for the apatite bone crystals. Crystallite size (d) was expressed in Angstrom units (Å). XPowder software was used to determine the XRD measurements.

2.8. Statistical Analyses

Bone mineral parameters were expressed as means ± standard error. The normal distribution and homogeneity of variances were verified by Shapiro-Wilk and Levene's tests. Differences between groups were assessed by parametric Student's *t*-tests. For data that were not normally distributed (i.e., Tb.Th and bend displacement), comparisons between groups were performed by non-parametric Mann Whitney U tests. Differences were considered significant at $p < 0.05$. Statistical analyses were performed using the SPSS 24.0 (SPSS Inc., Chicago, IL, USA) software package.

3. Results

3.1. Micro-Architectural Characteristics

Figure 2 displays micro-CT images (transversal–left and sagittal–right sections) showing the changes in the trabecular bone distribution in the alveolar region of rat mandibles from the control and lead-exposed groups. Micro-CT images of the lead-exposed (Figure 2: upper images) group showed a marked loss of trabecular bone distribution compared with those of the control group (Figure 2: lower images).

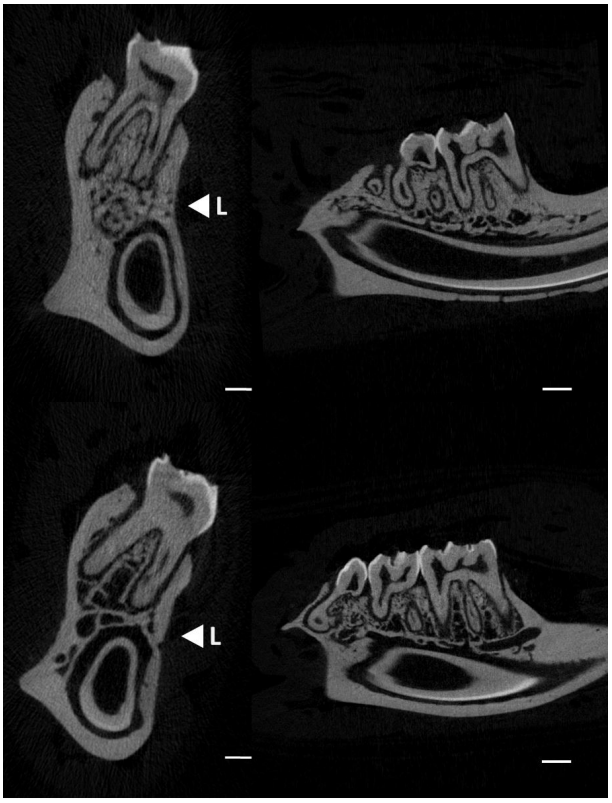

Figure 2. Micro-CT images showing the changes in alveolar bone in rat mandibles (transversal and sagittal sections) in the control (upper images) and lead exposure (lower images) groups. <L; direction for the mechanical load (three-point bending test). Scale bars: 1 mm.

The scanning electron images show the trabecular distribution of alveolar bone in the control and lead-exposed groups (Figure 3). These images display the bone structure of the mandible and the enlarged view of the first molar inter-radicular region. A relative decrease in trabecular bone distribution and higher porosity were observed in the lead-exposed group compared with the control group.

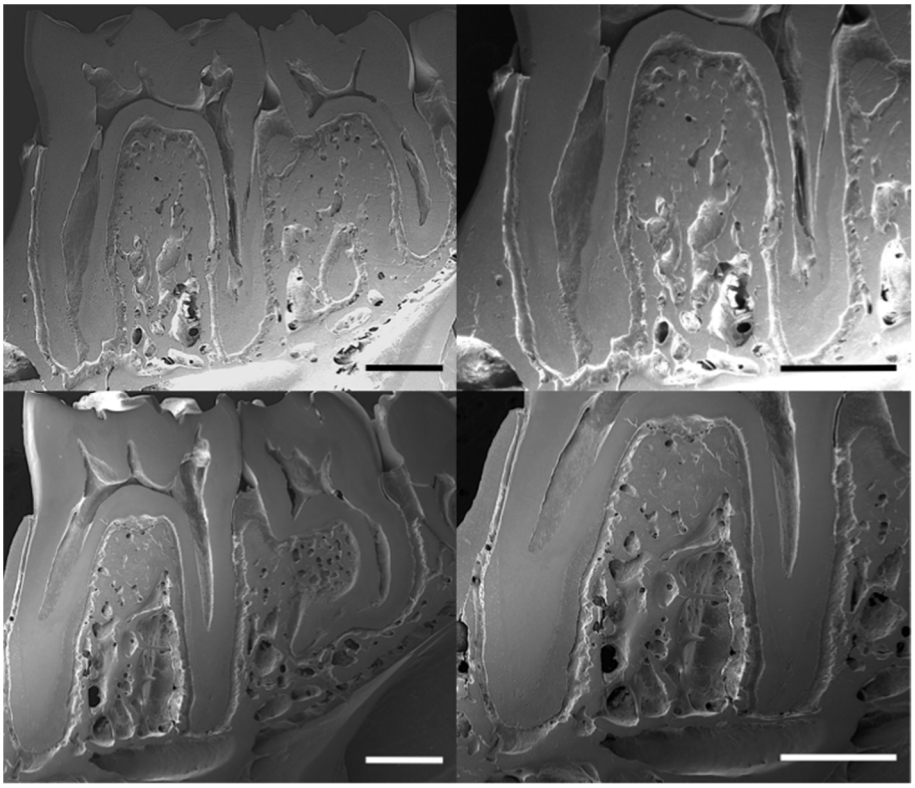

Figure 3. Scanning electron micrographs (SEM) showing the microstructural changes of alveolar bone in buccal axial cross-sections of rat mandibles in the control (upper row images) and lead-exposed (lower row images) groups. Scale bars: 1 mm.

The bone micro-architectural parameters obtained by micro-CT analyses are reported in Table 1. Trabecular parameters in the alveolar bone from lead-exposed rats showed a significant decrease in the bone volume (BV; $p = 0.019$), ratio of bone volume/total volume tissue (BV/TV; $p = 0.028$), and bone mineral density (BMD; $p = 0.014$) compared with the control group. In addition, a significantly higher number of trabeculae was observed in the control group (Tb.N; $p = 0.045$), although no significant differences in trabecular separation and thickness or connectivity density were observed between groups.

Table 1. Bone trabecular micro-architectural parameters obtained by micro-CT from rat mandibles in the chronic lead exposure ($n = 8$) and control ($n = 5$) groups. Values are expressed as means ± S.E.M. (N.S. = not significant).

	Control			Lead			*p* Value
TV (mm^3)	24.173	±	2.065	17.546	±	2.223	N.S.
BV (mm^3)	11.189	±	1.279	6.427	±	0.995	0.019
BV/TV (%)	46.056	±	3.030	35.945	±	2.394	0.028
BMD (mg/cm^3)	1142.60	±	7.68	1093.01	±	12.49	0.014
Tb.Th (mm)	0.111	±	0.005	0.102	±	0.004	N.S.
Tb.Sp (mm)	0.247	±	0.0167	0.227	±	0.0139	N.S.
Tb.N (1/mm)	4.128	±	0.206	3.504	±	0.168	0.045
Conn.Dn ($1/mm^3$)	157.07	±	30.26	138.54	±	18.85	N.S.

3.2. Mechanical Properties (Three-Point Bending Test)

The results of the three-point bending test are presented in Table 2. Lead exposure significantly decreased the displacement at failure in the alveolar region ($p = 0.002$) compared with the control group. No statistical differences were found for the maximal load resistance, although the mean was slightly higher in the lead exposure group.

Table 2. Three-point bending test in rat mandibles in the chronic lead exposure ($n = 8$) and control ($n = 5$) groups. Values are expressed as means ± S.E.M. (N.S. = not significant).

	Control			Lead			*p* Value
Bend displacement (mm)	2.28	±	0.20	1.30	±	0.15	0.008
Maximal bending Load (N)	85.90	±	2.25	87.04	±	5.28	N.S.

3.3. Bone Mineral Composition

Bone mineral compositional parameters obtained by the ICP-OES and ATR-FTIR analyses are presented in Table 3. Bone elemental results from ICP-OES indicated that the administered lead was deposited in the rat mandibles in significant loads (1.33 ± 0.08 μg/g). This result was expected, since blood lead levels reached a concentration of 40.56 ± 5.86 μg/dL in the lead-exposed group, versus 1.65 ± 0.59 μg/dL in the control group. The contents of Ca and P elements, as well as the Ca/P ratio, showed similar values between groups. On the other hand, the alveolar bone mineral in the control group had a higher carbonate content than the bone of the lead exposure group ($p = 0.004$), as determined by the ATR-FTIR analyses.

Table 3. Bone chemical parameters measured by ICP-OES and ATR-FTIR analyses of rat mandibles in the chronic lead exposure ($n = 8$) and control groups ($n = 5$). Values are expressed as means ± S.E.M (L.O.D. = limits of detection, N.S. = not significant).

	Control			Lead			*p* Value
ICP-OES analyses							
Pb μg/g		L.O.D.		1.33	±	0.08	
Ca (% d.w.)	24.26	±	0.94	24.25	±	0.12	N.S.
P (% d.w.)	11.06	±	4.26	11.03	±	1.47	N.S.
Ca/P	2.20	±	0.04	2.19	±	0.01	N.S.
ATR-FTIR analyses							
Degree mineralization	3.96	±	0.12	4.14	±	0.11	N.S.
Carbonate in bone mineral	0.31	±	0.008	0.28	±	0.006	0.004
Crystallinity index	0.71	±	0.01	0.76	±	0.03	N.S.

3.4. Crystalline Properties

The alveolar bone mineral crystallinity, measured as apatite crystallite size, is presented in Figure 4. Alveolar bone from the lead exposure group showed a significantly increased crystallite size (172 ± 2.5 Å) compared with the control group (150 ± 8.3 Å; $p = 0.011$).

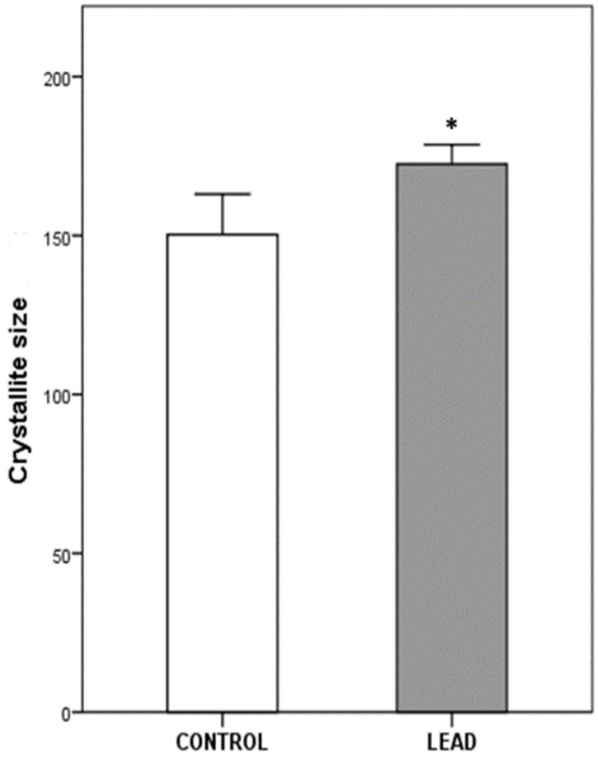

Figure 4. Crystallite size measurements of apatite crystals in the alveolar bone of the control (n = 5) and lead exposure (n = 8) groups. Values (Å) are expressed as means ± S.E.M. Asterisk indicates statistical differences between groups ($p < 0.05$).

4. Discussion

Lead exposure is related to various defective skeletal growth processes and bone mineral disturbances, ultimately leading to bone diseases such as osteoporosis. Many studies have shown the potential impact of lead poisoning on bone mineralization, especially in long bones [5,11,24]. However, few studies have assessed the specific effects of lead exposure on alveolar bone mineralization. The current study demonstrated that chronic lead exposure altered alveolar bone characteristics not only at the morphological level but also in its mineral chemistry and crystalline properties. These alterations in the trabecular morphology, microstructure, and mineral composition are all critical factors for bone material quality, as they affect the mechanical properties of bone tissue.

Previous studies have shown that lead exposure can reduce mineral density and modify bone mineral and matrix composition due to an increased rate of bone turnover [10]. Chemical alteration in bone apatite may also affect various physiological processes related to lead toxicity [6,25]. Alveolar bone shows a high rate of bone resorption and redeposition, as its formation is closely linked to the development of each new tooth [26]. In our study, the observed decrease in carbonate content and greater crystallinity in alveolar bone mineral in rats in the lead-exposed group suggest an alteration in bone turnover rate. Newly deposited bone mineral is characterized by low crystallinity and high carbonate content of apatite crystals. As bone mineral matures, its carbonate content decreases as its crystallinity increases [19,27]. Thus, these results may also indicate that lead exposure produced a reduction in bone resorption, which can impair new bone mineral formation, as well as an increased bone tissue age and bone mineral maturation. This alteration can also prevent new apatite crystal formation, resulting in a population containing a higher proportion of larger crystals (i.e., higher crystallite size). These crystalline characteristics determine other critical properties of bone mineral (e.g., solubility rates and orientation degree of collagen fibrils). Previous studies reported that lead can substitute calcium in the hydroxyapatite crystal, forming a lead apatite structure [28,29]. The Ca^{2+} ionic substitution

by other divalent cations (e.g., Pb^{2+}) in the HAp crystal lattice also affects the crystallization kinetics and thermodynamics and, consequently, the stability of the mineral under biological conditions [30]. In the current study, chronic exposure to lead was associated with an accumulation of the Pb cation in the HAp crystals, provoking a significant alteration in the crystallinity properties observed by X-ray diffraction, expressed as an increase in crystallite size. Previous research observed that lead apatite has larger cell parameters (e.g., increased *c-axis* dimension) than analogous calcium compounds [31], as evidenced by the larger ionic radius of Pb^{2+} (1.37 Å) versus Ca^{2+} (1.20 Å). These observations suggest that there is a subtle difference in the apatite microstructure (i.e., crystal size domains) influence of calcium to lead substitution on bone mineral, which can be attributed to the alteration in the stereochemical activity caused by the effects of lead exposure.

Micro-CT analyses allow the study of morphological changes at the micro-architectural level in bone health and disease [32]. Here, we focused on the characterization of the trabecular organization in the alveolar bone region, as it constitutes the main structure in this specific non-weight bearing bone [1]. Moreover, alveolar bone is clinically quite important, as it represents the most metabolically active type of bone involved in dentition development [2]. The micro-CT results in the current research showed a significant decrease in the bone mineral density (BMD) and bone volume to tissue volume ratio (BV/TV) in the trabecular bone of lead-exposed rats compared with the control group. SEM images also confirmed this impairment in the trabecular structure of the alveolar bone. These observations showed higher porosity and a decrease in trabecular density in the lead-exposed group, particularly in the inter-radicular region of the mandibular molars. Previous studies showed the effect of lead exposure on decreased bone density in both cortical and trabecular bone in rat femurs [10,33]. These effects indicate a similar mechanism of bone maturation normally associated with osteoporosis [34,35]. In fact, the decrease of the trabecular microarchitecture characteristics in alveolar bone has been related to increased incidence of osteoporosis and risk of fractures [35–37]. Furthermore, the trabecular bone in the alveolar region showed a decrease in the number of trabeculae in the lead exposure group. Similar alterations have been reported in osteoporosis, in which a marked reduction of the trabecular bone volume, as well as a reduction in the thickness and number of trabecular, was observed [32,38]. The process of bone remodelling comprises a number of cellular events in which trabecular sites, due to their high surface-to-volume ratio, were more commonly affected by the dysregulation in bone turnover processes [39]. The alteration of the bone metabolism caused by lead exposure [6,40] may be related to the deterioration of the trabecular characteristics in alveolar bone, which resembles bone mineral loss [33]. Moreover, mineral alterations in the alveolar region are associated with a physiological disorder that can lead to a structural disorder with important mechanical implications.

Bone mechanical properties are largely influenced by the intrinsic characteristics of their components and the quantity and spatial distribution of the mineralized structure [41]. Previous research has shown a decrease in maximum and failure moments in rat femurs exposed to lead compared with controls [10,24]. Additionally, published research from our laboratory showed reduced biomechanical properties of the mandibles of rats exposed to lead for 90 days, mainly due to an impaired geometrical distribution of the bone and poorer material properties [42,43]. From a mechanical point of view, bone strength depends mainly on the amount of bone mineral content and the arrangement of the trabeculae [44]. It has been previously stated that lead exposure is capable of reducing the quality of trabecular bone (i.e., decreased BMD), directly affecting its ability to support mechanical stress, which was corroborated by the results obtained from the three-point bending test. Our mechanical analyses showed less flexibility (i.e., bending displacement) to failure in the alveolar region of the mandibles from rats exposed to lead. Thus, as a result of the reduced structural characteristics of the trabeculae (e.g., trabecular thickness and number of trabeculae), the bone becomes brittle, with a decrease in the extension to the point of fracture and the flexural strength [36,45]. These observations are consistent

with our previous suggestion of an osteoporotic characteristic of bone alterations due to lead exposure [37]. In addition, the mechanical integrity of the mandibles may be also related to the mineral compositional and microstructural properties of the bone (i.e., carbonate mineral content and crystallite size), as discussed above.

Numerous studies have demonstrated the association between lead exposure and bone mineral disorders, including osteopenia and osteoporosis [7,17,46]. Even though the toxic limit of Pb in the blood is considered to be 10 ug/dL in adults and 5 μg/dL for children (according to the Centers for Disease Control and Prevention, Atlanta, USA), values of blood lead level > 8 μg/dL were correlated with an increased risk of bone fractures in older women [47]. In our study, the lead exposure group reached blood lead levels of 40.56 ± 5.86 μg/dL, which are considered environmentally relevant exposures and can be extrapolated to human populations living near metallurgical complexes (e.g., populations inhabiting regions of important mining resources such as La Oroya, Peru) and occupationally exposed workers, as reported in the United States [48]. At the metabolic level, lead intoxication can directly and indirectly alter many features of bone cell functions, disrupting their ability to react to hormonal regulation and/or modifying the circulating levels of those hormones (particularly 1,25-dihydroxyvitamin D3) that modulate their actions [46]. In addition, lead exposure may affect calcium homeostasis or substitute at the active sites of the calcium messenger systems in many physiological regulations [25]. Thus, lead toxicity in bone is related to the various coupled effects produced in the regulatory processes of bone turnover mechanisms (i.e., bone remodelling) that ultimately affect the mineral properties of the tissue [40]. In any case, further research is necessary to obtain information on the altered rate of bone remodelling and mineralization kinetics associated with chronic lead exposure and abnormalities in alveolar bone. In addition, the progressive alveolar bone loss in lead exposure has significant dental implications since it may promote the appearance of periodontal disease [49,50]. These alterations in the bone mandible structure compromise oral health status, increasing the risk of fracture and affecting the physiological function of the alveolar bone during the development of the dentition.

5. Conclusions

This study showed that chronic lead exposure induces alterations in bone mineral composition and its crystalline properties in the alveolar bone of rat mandibles. In rats exposed to lead, there was a reduction in carbonate content and an increase in apatite crystallinity. At the morphological level, lead exposure induced notable changes in the reduction of trabecular thickness and bone mineral density. These changes suggest a possible alteration in bone remodelling mechanisms that affect the organization of the trabecular architecture and, consequently, the mechanical properties of the mandibles. These disruptions in alveolar bone mineralization caused by lead exposure may compromise the maintenance of the mechanical stability and normal development of the dentition. Lead exposure is likely to remain a major public health issue, especially in developing countries, where the persistence of this contaminant in the environment due to industrialization is still a major concern. Regarding oral health, ongoing public health initiatives are needed since lead exposure represents a risk for mandibular structure alterations that may result in fractures and inadequate dentition development, as demonstrated in the current research.

Author Contributions: Conceptualization, P.Á.-L. and A.R.T.; methodology, C.-M.L., M.P.M., M.I.C., and A.R.T.; software, P.Á.-L. and C.B.-R.; validation, A.B.R.-N., S.G.-L., and P.Á.-L.; formal analysis, C.B.-R. and P.Á.-L.; investigation, P.Á.-L., M.P.M., A.R.T., and C.B.-R.; resources, P.Á.-L., A.B.R.-N., S.G.-L., M.P.M., M.I.C., C.-M.L., A.P.-H., and A.R.T.; data curation, P.Á.-L., C.B.-R., A.P.-H., and A.R.T.; writing—original draft preparation, P.Á.-L. and A.R.T.; writing—review and editing, C.B.-R., C.-M.L., M.P.M., M.I.C., A.B.R.-N., S.G.-L., A.P.-H., and A.R.T.; visualization, C.B.-R. and P.Á.-L.; supervision, A.R.T.; project administration, A.B.R.-N. and M.P.M.; funding acquisition, A.B.R.-N., P.Á.-L., and A.R.T. All authors have read and agreed to the published version of the manuscript.

Funding: This research was funded by MICINN-CGL2011-25906 (Spain) and UBACYT-20020150100006BA (Argentina) grants.

Institutional Review Board Statement: The study was conducted according to the guidelines of the Declaration of Helsinki, and approved by the Institutional Review Board (or Ethics Committee) of University of Buenos Aires (protocol code: 23-11/06/2012).

Informed Consent Statement: Not applicable.

Data Availability Statement: Data available on request from the corresponding author.

Acknowledgments: We acknowledge CIC (University of Granada) and SCT (University of Oviedo) and the staff for their technical support and assistance. The authors thank Vanessa Loredo for the micro-CT data analyses and David Garofano for the optical microscopy images. The authors would like to thank Jeremy Dunn for English proofreading.

Conflicts of Interest: The authors declare no conflict of interest.

References

1. Chu, T.-M.G.; Liu, S.S.Y.; Babler, W.J. Craniofacial biology, orthodontics, and implants In *Basic and Applied Bone Biology*; Burr, D.B., Allen, M.R., Eds.; Elsevier-Academic Press: Amsterdam, The Netherlands, 2014; pp. 225–242, doi:10.1016/B978-0-12-416015-6.00011-3.
2. Almela, T.; Brook, I.M.; Moharamzadeh, K. Bone tissue engineering in maxillofacial region. In *Biomaterials for Oral and Dental Tissue Engineering*; Woodhead Publishing: Cambridge, UK, 2017; pp. 3–6, doi:10.1016/B978-0-08-100961-1.00023-2.
3. Eriksen, E.F.; Vesterby, A.; Kassem, M.; Melsen, F.; Mosekilde, L. Bone remodeling and bone structure. In *Physiology and Pharmacology of Bone*; Mundy, G.R., Martin, T.J., Eds.; Springer-Verlag: Berlin, Germany, 1993; pp. 67–109, doi:10.1007/978-3-642-77991-6.
4. LeGeros, R.Z. Calcium phosphates in oral biology and medicine. *Monogr. Oral Sci.* **1991**, *15*, 1–201.
5. Alvarez-Lloret, P.; Lee, C.M.; Conti, M.I.; Terrizzi, A.R.; González-López, S.; Martínez, M.P. Effects of chronic lead exposure on bone mineral properties in femurs of growing rats. *Toxicology* **2017**, *37*, 64–72, doi:10.1016/j.tox.2016.11.017.
6. Berglund, M.; Akesson, A.; Bjellerup, P.; Vahter, M. Metal-bone interactions. *Toxicol. Lett.* **2000**, *112–113*, 219–225, doi:10.1016/S0378-4274(99)00272-6.
7. Berlin, K.; Gerhardsson, L.; Börjesson, J.; Lindh, E.; Lundström, N.; Schütz, A.; Skerfving, S.; Edling, C. Lead intoxication caused by skeletal disease. *Scand. J. Work Environ. Health* **1995**, *21*, 296–300, doi:10.5271/sjweh.42.
8. Ronis, M.J.J.; Aronson, J.; Gao, G.G.; Hogue, W.; Skinner, R.A.; Badger, T.M.; Lumpkin, C.K., Jr. Skeletal effects of developmental lead exposure in rats. *Toxicol. Sci.* **2001**, *62*, 321–329, doi:10.1093/toxsci/62.2.321.
9. Gangoso, L.; Álvarez-Lloret, P.; Rodríguez-Navarro, A.B.; Mateo, R.; Hiraldo, F.; Donázar, J.A. Long-term effects of lead poisoning on bone mineralization in vultures exposed to ammunition sources. *Environ. Pollut*. **2009**, *157*, 569–574, doi:10.1016/j.envpol.2008.09.015.
10. Monir, A.U.; Gundberg, C.M.; Yagerman, S.E.; van der Meulen, M.C.; Budell, W.C.; Boskey, A.L.; Dowd, T.L. The effect of lead on bone mineral properties from female adult C57/BL6 mice. *Bone* **2010**, *47*, 888–894, doi:10.1016/j.bone.2010.07.013.
11. Rodríguez-Estival, J.; Álvarez-Lloret, P.; Rodríguez-Navarro, A.B.; Mateo, R. Chronic effects of lead (Pb) on bone properties in red deer and wild boar: Relationship with vitamins A and D3. *Environ. Pollut.* **2013**, *174*, 142–149, doi:10.1016/j.envpol.2012.11.019.
12. Boskey, A.L.; Mendelsohn, R. Infrared spectroscopic characterization of mineralized tissues. *Vib. Spectrosc*. **2005**, *38*, 107–114, doi:10.1016/j.vibspec.2005.02.015.
13. Rey, C.; Combes, C.; Drouet, C.; Glimcher, M.J. Bone mineral: Update on chemical composition and structure. *Osteoporosis Int.* **2009**, *20*, 1013–1021, doi:10.1007/s00198-009-0860-y.
14. Sanchez-Rodriguez, E.; Benavides-Reyes, C.; Torres, C.; Dominguez-Gasca, N.; Garcia-Ruiz, A.I.; Gonzalez-Lopez, S.; Rodriguez-Navarro, A.B. Changes with age (from 0 to 37 D) in tibiae bone mineralization, chemical composition and structural organization in broiler chickens. *Poult. Sci.* **2019**, *98*, 5215–5225, doi:10.3382/ps/pez363.
15. Shah, F.A.; Ruscsák, K.; Palmquist, A. 50 years of scanning electron microscopy of bone—A comprehensive overview of the important discoveries made and insights gained into bone material properties in health, disease, and taphonomy. *Bone Res.* **2019**, *7*, 15, doi:10.1038/s41413-019-0053-z.
16. Dempster, D.W.; Compston, J.E.; Drezner, M.K.; Glorieux, F.H.; Kanis, J.A.; Malluche, H.; Meunier, P.J.; Ott, S.M.; Recker, R.R.; Parfitt, A.M. Standardized nomenclature, symbols, and units for bone histomorphometry: A 2012 update of the report of the ASBMR Histomorphometry Nomenclature Committee. *J. Bone Miner. Res.* **2013**, *28*, 2–17, doi:10.1002/jbmr.1805.
17. Hamilton, J.D.; O'Flaherty, E.J. Effects of lead exposure on skeletal development in rats. *Fundam. Appl. Toxicol.* **1994**, *22*, 594–604, doi:10.1006/faat.1994.1066.
18. Bouxsein, M.L.; Boyd, S.K.; Christiansen, B.A.; Guldberg, R.E.; Jepsen, K.J.; Müller, R. Guidelines for assessment of bone microstructure in rodents using micro-computed tomography. *J. Bone Miner. Res.* **2010**, *25*, 1468–1486, doi:10.1002/jbmr.141.

19. Ou-Yang, H.; Paschalis, E.P.; Mayo, W.E.; Boskey, A.L.; Mendelsohn, R. Infrared microscopic imaging of bone: Spatial distribution of CO3(2−). *J. Bone Miner. Res.* **2001**, *16*, 893–900, doi:10.1359/jbmr.2001.16.5.893.
20. Rey, C.; Collins, B.; Goehl, T.; Dickson, I.R.; Glimcher, M.J. The carbonate environment in bone mineral: A resolution-enhanced fourier transform infrared spectroscopy study. *Calcif. Tissue Int.* **1989**, *45*, 157–164, doi:10.1007/BF02556059.
21. Miller, L.S.; Vairavamurthy, V.; Chance, M.R.; Mendelsohn, R.; Paschalis, E.P.; Betts, F.; Boskey, A.L. In situ analysis of mineral content and crystallinity in bone using infrared micro-spectroscopy of the v4 PO4-3 vibration. *Biochim. Biophys. Acta* **2001**, *1527*, 11–19, doi:10.1016/s0304-4165(01)00093-9.
22. Schreiner, W.N.; Jenkins, T. Profile fitting for quantitative. Analysis in X-ray powder diffraction. *Adv. X-ray Anal.* **1983**, *26*, 141.
23. Klug, H.P.; Alexander, L.E. *X-ray Diffraction Procedures*; John Willey: New York, NY, USA, 1959.
24. Olchowik, G.; Widomska, J.; Tomaszewski, M.; Gospodarek, M.; Tomaszewska, M.; Jagiełło-Wójtowicz, E. The influence of lead on the biomechanical properties of bone tissue in rats. *Ann. Agric. Environ. Med.* **2014**, *21*, 278–281, doi:10.5604/1232-1966.1108591.
25. Pounds, J.G. Effect of lead intoxication on calcium homeostasis and calcium-mediated cell function: A review. *Neurotoxicology* **1984**, *5*, 295–331.
26. Huja, S.S.; Fernandez, S.A.; Hill, K.J.; Li, Y. Remodeling dynamics in the alveolar process in skeletally mature dogs. *Anat. Rec. A. Discov. Mol. Cell. Evol. Biol.* **2006**, *288*, 1243–1249, doi:10.1002/ar.a.20396.
27. Donnelly, E.; Boskey, A.L.; Baker, S.P.; van der Meulen, M.C. Effects of tissue age on bone tissue material composition and nanomechanical properties in the rat cortex. *J. Biomed. Mater. Res. A* **2010**, *92*, 1048–1056, doi:10.1002/jbm.a.32442.
28. Brès, E.F.; Voegel, J.C.; Barry, J.C.; Waddington, W.G.; Frank, R.M. Feasibility study for the detection of lead substitution sites in the hydroxyapatite crystal structure using high-resolution electron microscopy (HREM) at optimum focus. *J. Appl. Cryst.* **1986**, *19*, 168–173, doi:10.1107/S0021889886089719.
29. McConnell, D. *Apatite, Its Crystal Chemistry, Mineralogy and Utilisation*; Springer: New York, NY, USA, 1973; doi:10.1007/978-3-7091-8314-4.
30. Cacciotti, I. Cationic and Anionic Substitutions in Hydroxyapatite. In *Handbook of Bioceramics and Biocomposites*; Antoniac, I., Ed.; Springer: Cham, Switzerland, 2016; pp. 145–211, doi:10.1007/978-3-319-12460-5_7.
31. Kim, J.Y.; Fenton, R.R.; Hunter, B.A.; Kennedy, B.J. Powder diffraction studies of synthetic calcium and lead apatites. *Aust. J. Chem.* **2000**, *53*, 679–686, doi:10.1071/CH00060.
32. Chappard, D.; Baslé, M.-F.; Legrand, E.; Audran, M. Trabecular bone microarchitecture: A review. La microarchitecture de l'os trabéculaire: Une revue. *Morphologie* **2008**, *92*, 162–170, doi:10.1016/j.morpho.2008.10.003.
33. Sheng, Z.; Wang, S.; Zhang, X.; Li, X.; Zhang, Z. Long-Term Exposure to Low-Dose Lead Induced Deterioration in Bone Microstructure of Male Mice. *Biol. Trace Elem. Res.* **2020**, *195*, 491–498, doi:10.1007/s12011-019-01864-7.
34. Jiang, G.; Matsumoto, H.; Fujii, A. Mandible bone loss in osteoporosis rats. *J. Bone Miner. Metab.* **2003**, *21*, 388–395, doi:10.1007/s00774-003-0433-7.
35. Moriya, Y.; Ito, K.; Murai, S. Effects of experimental osteoporosis on alveolar bone loss in rats. *J. Oral Sci.* **1998**, 40:171–175, doi:10.2334/josnusd.40.171.
36. Jiang, G.; Matsumoto, H.; Hori, M.; Gunji, A.; Hakozaki, K.; Akimoto, Y.; Fujii, A. Correlation among geometric, densitometric, and mechanical properties in mandible and femur of osteoporotic rats. *J. Bone Miner. Metab.* **2008**, *26*, 130–137, doi:10.1007/s00774-007-0811-7.
37. Payne, J.B.; Reinhardt, R.A.; Nummikoski, P.V.; Patil, K.D. Longitudinal alveolar bone loss in postmenopausal osteoporotic/osteopenic women. *Osteoporos Int.* **1999**, *10*, 34–40, doi:10.1007/s001980050191.
38. Francis, R.M.; Peacock, M.; Marshall, D.H.; Horsman, A.; Aaron, J.E. Spinal osteoporosis in men. *Bone Miner.* **1989**, *5*, 347–357, doi:10.1016/0169-6009(89)90012-3.
39. Aaron, J.E.; Johnson, D.R.; Paxton, S.; Kanis, J.A. Secondary osteoporosis and the microanatomy of trabecular bone. *Clin. Rheumatol.* **1989**, *8*, 84–88, doi:10.1007/BF02207240.
40. Brito, J.A.A.; Costa, I.M.; Maia e Silva, A.; Marques, J.M.S.; Zagalo, C.M.; Cavaleiro, I.I.B.; Fernandes, T.A.P.; Goncalves, L.L. Changes in bone Pb accumulation: Cause and effect of altered bone turnover. *Bone* **2014**, *64*, 228–234, doi:10.1016/j.bone.2014.04.021.
41. Ferretti, J.L. Biomechanical Properties of Bone. In *Bone Densitometry and Osteoporosis*; Genant, H.K., Guglielmi, G., Jergas, M., Eds.; Springer: Berlin/Heidelberg, Germany, 1998; pp. 143–149.
42. Conti, M.I.; Bozzini, C.; Facorro, G.B.; Lee, C.M.; Mandalunis, P.M.; Piehl, L.L.; Piñeiro, A.E.; Terrizzi, A.R.; Martínez, M.P. Lead bone toxicity in growing rats exposed to chronic intermittent hypoxia. *Bull. Environ. Contam. Toxicol.* **2012**, *89*, 693–698, doi:10.1007/s00128-012-0753-1.
43. Conti, M.I.; Terrizzi, A.R.; Lee, C.M.; Mandalunis, P.M.; Bozzini, C.; Piñeiro, A.E.; Martínez, M.P. Effects of lead exposure on growth and bone biology in growing rats exposed to simulated high altitude. *Bull. Environ. Contam. Toxicol.* **2012**, *88*, 1033–1037, doi:10.1007/s00128-012-0602-2.
44. Osterhoff, G.; Morgan, E.F.; Shefelbine, S.J.; Karim, L.; McNamara, L.M.; Augat, P. Bone mechanical properties and changes with osteoporosis. *Injury* **2016**, *47 (Suppl. 2)*, S11–S20, doi:10.1016/S0020-1383(16)47003-8.
45. Morgan, E.F.; Unnikrisnan, G.U.; Hussein, A.I. Bone Mechanical Properties in Healthy and Diseased States. *Ann. Rev. Biomed.* **2018**, 20, 119–143, doi:10.1146/annurev-bioeng-062117-121139.

46. Pounds, J.G.; Long, G.J.; Rosen, J.F. Cellular and molecular toxicity of lead in bone. *Environ. Health Perspect.* **1991**, *91*, 17–32, doi:10.1289/ehp.919117.
47. Khalil, N.; Cauley, J.A.; Wilson, J.W.; Talbott, E.O.; Morrow, L.; Hochberg, M.C.; Hillier, T.A.; Muldoon, S.B.; Cummings, S.R. Relationship of blood lead levels to incident non spine fractures and falls in older women: The study of osteoporotic fractures. *J. Bone Miner. Res*. **2008**, *23*, 1417–1425.
48. Centers for Disease Control and Prevention (CDC). Very high blood lead levels among adults—United States, 2002–2011. *MMWR Morb. Mortal. Wkly. Rep*. **2013**, 62, 967–971.
49. Terrizzi, A.R.; Fernandez-Solari, J.; Lee, C.M.; Bozzini, C.; Mandalunis, P.M.; Elverdin, J.C.; Conti, M.I.; Martínez, M.P. Alveolar bone loss associated to periodontal disease in lead intoxicated rats under environmental hypoxia. *Arch. Oral. Biol.* **2013**, 58, 1407–1414, doi:10.1016/j.archoralbio.2013.06.010.
50. Tort, B.; Choi, Y.H.; Kim, E.K.; Jung, Y.S.; Ha, M.; Song, K.B.; Lee, Y.E. Lead exposure may affect gingival health in children. *BMC Oral Health* **2018**, *18*, 79, doi:10.1186/s12903-018-0547-x.